

# A Novel Method to Fabricate Silicon Nanowire $p$ – $n$ Junctions by a Combination of Ion Implantation and in-situ Doping

Pratyush Das Kanungo · Reinhard Kögler ·  
Peter Werner · Ulrich Gösele · Wolfgang Skorupa

Received: 9 October 2009 / Accepted: 14 October 2009 / Published online: 8 November 2009  
© to the authors 2009

**Abstract** We demonstrate a novel method to fabricate an axial  $p$ – $n$  junction inside  $\langle 111 \rangle$  oriented short vertical silicon nanowires grown by molecular beam epitaxy by combining ion implantation with in-situ doping. The lower halves of the nanowires were doped in-situ with boron (concentration  $\sim 10^{18} \text{ cm}^{-3}$ ), while the upper halves were doubly implanted with phosphorus to yield a uniform concentration of  $2 \times 10^{19} \text{ cm}^{-3}$ . Electrical measurements of individually contacted nanowires showed excellent diode characteristics and ideality factors close to 2. We think that this value of ideality factors arises out of a high rate of carrier recombination through surface states in the native oxide covering the nanowires.

**Keywords** Nanowire ·  $p$ – $n$  Junction · Ion implantation · In-situ doping · Electrical properties

## Introduction

In order to make use of silicon nanowires (Si NWs) [1] in nano-devices, selective doping to form  $p$ – $n$  junctions or  $p$  and  $n$  wells is a necessity. Till date, a host of devices with selectively doped Si NWs have been demonstrated [1, 2]. Out of them, axial  $p$ – $n$  [3] and  $p$ – $n$ – $i$  [4] junction in Si NWs have shown the potential to be used as solar cells. However, axial  $p$ – $n$  junctions in NWs grown by the vapor–

liquid–solid (VLS) technique have mostly been fabricated by purely in-situ doping [3, 5, 6]. It has been observed that a pure in-situ doping to fabricate an axial junction may result in unwanted lateral doping [6] due to unavoidable dopant incorporations through the NW sidewalls by vaporsolid (VS) growth. On the other hand, ion implantation [7] which is the most widely used doping technique in very large scale integration (VLSI) fabrication can form well-confined doped regions when appropriately used with masking. Ion implantation has been used to fabricate the doped source and drain contacts [8] as well as the channel [9] in Si NW-based field effect transistors (FETs). But one of the principal reasons for not extensively using ion implantation to fabricate axial junctions in vertical NWs is possible irrecoverable implantation damages [10] that were observed in other low dimensional structures such as a FinFET [11]. However, we have shown [12] that by choosing appropriate ion doses and energies, it is possible to uniformly dope vertical Si NWs of diameter in the range of 100 nm without leaving any residual structural defects in them. Separately, we have also demonstrated in-situ doping of molecular beam epitaxy (MBE)-grown Si NWs [13]. S. Hoffmann et al. [14] have realized a  $p$ – $n$  junction in a Si NW purely by ion implantation. However, co-diffusion of acceptors and donors during annealing after such dual implantations of different ions (boron and phosphorus) often lead to the formation of acceptor–donor complexes [15, 16] that can anomalously increase the solubility of the donors in the acceptor-rich segments, thus affecting the  $p$ – and  $n$ – profiles.

In this paper, we demonstrate a novel approach to form an axial  $p$ – $n$  junction in a Si NW by combining the above-mentioned ex-situ and in-situ doping techniques. First, we do a modulated in-situ doping with boron by homogeneously doping the lower half of the NW to make it  $p$ -type.

P. D. Kanungo (✉) · P. Werner · U. Gösele  
Max Planck Institute of Microstructure Physics,  
Weinberg 2, 06120 Halle, Germany  
e-mail: kanungo@mpi-halle.de

R. Kögler · W. Skorupa  
Forschungszentrum Dresden, Rossendorf, FWIM,  
01314 Dresden, Germany

The upper half of the NW is kept intrinsic (*i*-type) by simply switching off the boron source. This intrinsic upper half is subsequently converted to *n*-type by implanting it with phosphorus. We present the details of the fabrication process, the expected dopant profiles in the NW, and electrical characterization of individual NW *p*–*n* diodes and explain their typical current–voltage (*I*–*V*) curves.

### Experimental Details

Basics of the growth process including the mechanism of Si NW growth by MBE using Au seeds have already been reported earlier [17]. The NWs were grown on 5'' *p*-type (boron doped, 5–10 Ω-cm) Si <111> wafers. A B-doped (B concentration  $\sim 10^{18}$  cm $^{-3}$ ) Si buffer layer was grown first on a RCA-cleaned wafer at 525°C in order to provide a clean surface for NW growth and increase the density of the NWs. Afterward, a 1–2-nm thick Au film was deposited in-situ at the same temperature. The Au film subsequently broke into Au droplets to serve as the NW growth initiator [17]. Immediately after this step, Si and B were co-evaporated for 45 min (B concentration  $\sim 10^{18}$  cm $^{-3}$ ). At 45 min, the B source was switched off, while the Si source was kept on 45 min longer. Such a recipe should result in B-doped—intrinsic (*p*–*i*) type NWs, since the boron diffusion in silicon is negligible at 525°C [7], i.e., the B atoms incorporated in the lower half will not diffuse into the upper half of the NW. Imamura et al. [18] verified this with Raman measurements on NWs grown by chemical vapor deposition (CVD) following a similar recipe as ours.

Figure 1 illustrates the different steps, accompanied by scanning electron microscope (SEM) images, to fabricate Si NW *p*–*n* diodes from the as-grown *p*–*i* NWs. The average length of our as-grown *p*–*i* NWs amounted to 300 nm and diameter to 125 nm (see Fig. 1a, b). As gold can act as an effective phosphorus ion stopper because of its heavy mass compared to phosphorus, the Au caps on top of the NWs were removed (Fig. 1c) by an aqueous solution of KI and  $I_2$ , a standard Au etchant. This resulted in the reduction in the average length of the NWs to around 260 nm (Fig. 1d). Before the implantations, the samples were spin coated using a spin-on-glass (SOG) silicon dioxide (Silicafilm, Emulsitone Co.) for 30 s at 3,000 rpm. This thereby protected the substrate (Fig. 1e) and the B-doped lower segment of the NWs from being implanted with P ions from the side. This step effectively eliminates the possibility of lateral doping that is almost unavoidable in purely in-situ doping of NWs successively by two different dopants [6]. A two-step implantation of phosphorus ions at room temperature was used to obtain a rectangular dopant profile. The implantation energies were 45 and 25 keV corresponding to doses of  $1.3 \times 10^{14}$  and

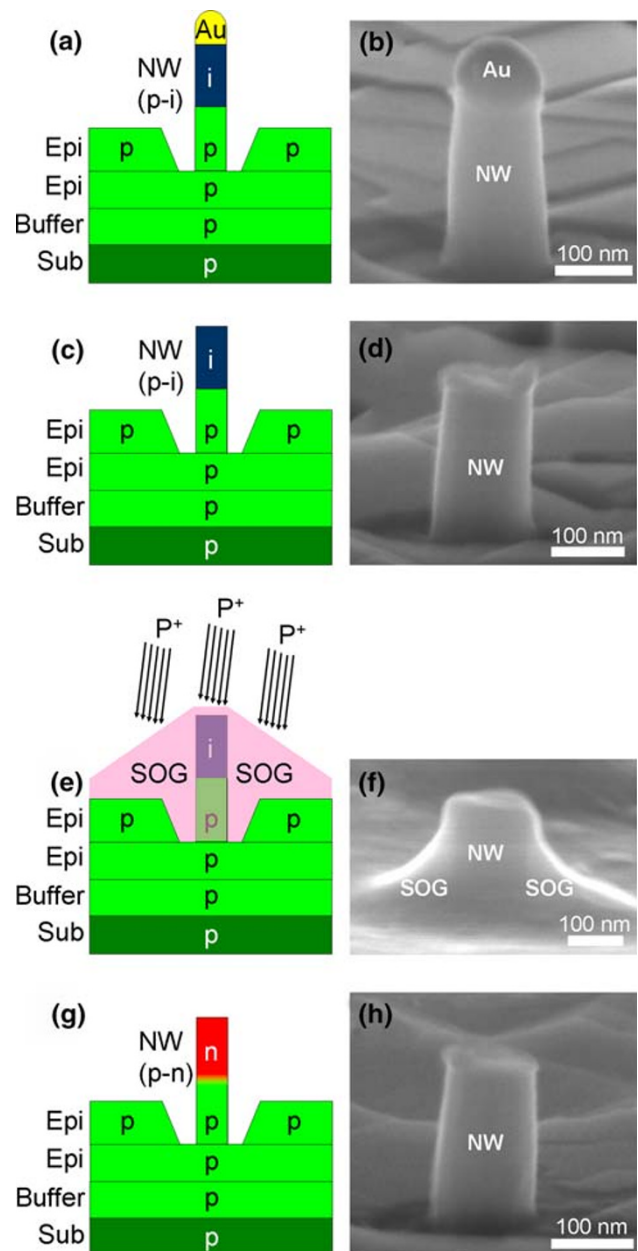


**Fig. 1** The scheme of fabricating axial *p*–*n* junction Si NWs—**a** An as-grown *p*–*i* NW **b** scanning electron microscope (SEM) image of an as-grown *p*–*i* NW. **c** A NW with the Au cap removed **d** SEM image of a NW with the Au cap removed **e** P ion implantation on a NW coated with the spin-on-glass (SOG) silicon dioxide. The top intrinsic part is converted to *n*-type **f** SEM image of an SOG-coated NW. **g** A *p*–*n* junction NW after the P ion implantation and removal of the SOG. **h** SEM image of a *p*–*n* junction NW

$3.2 \times 10^{13}$  cm $^{-2}$ , respectively. The NWs were tilted by 7° with respect to the impinging ions (Fig. 1e) to reduce ion channeling [7]. The implanted NWs were subsequently annealed by rapid thermal annealing (RTA) at 850°C for 30 s in Ar atmosphere. Afterward, the SOG was removed using an HF-dip resulting in the NW *p*–*n* diodes as shown in Fig. 1g (corresponding SEM image in Fig. 1h).

## Results and Discussions

We illustrate the formation of an axial  $p$ - $n$  junction in a NW in Fig. 2. Figure 2a shows the SEM image of a  $p$ - $n$  junction NW. Figure 2b shows the expected phosphorus concentration profile along the length of the NW simulated by the transport of ions in matter (TRIM) code [19] as well as the expected B concentration profile that results from the in-situ doping. The B profile was taken from the secondary ion mass spectrometry (SIMS) measurements reported earlier [13]. For simplicity, we considered the  $p$ - $n$  junction formed in Fig. 2b to be an abrupt one. Assuming full activation of the dopants, i.e., number of donors ( $N_D$ ) =  $2 \times 10^{19} \text{ cm}^{-3}$  (the peak P concentration) and number of acceptors ( $N_A$ ) =  $10^{18} \text{ cm}^{-3}$  (the peak B concentration), we calculated the depletion width [20] as 40 nm. This value is significantly smaller than the average

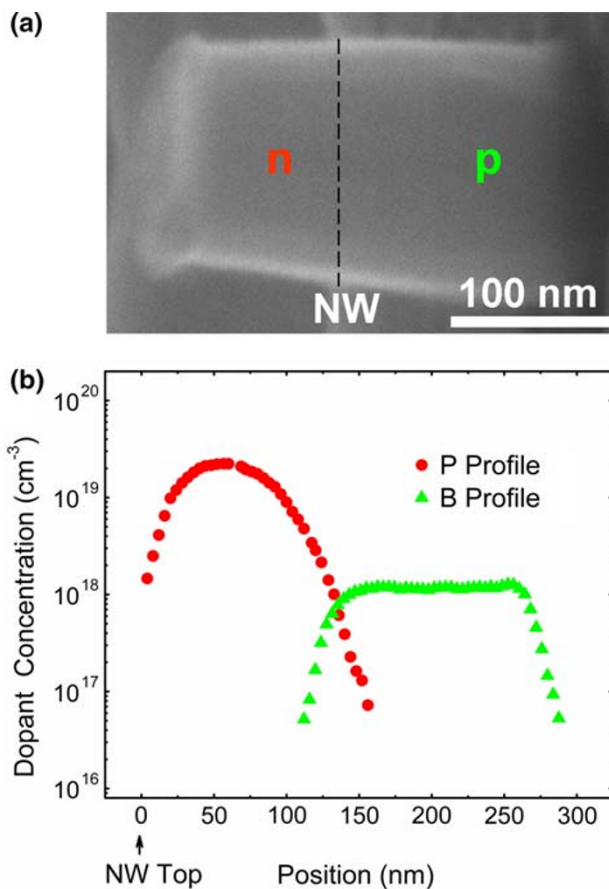


**Fig. 2** An illustration of how the  $p$ - $n$  junction is formed in a Si NW. **a** An SEM image of a NW indicating the  $p$ - and  $n$ -regions. **b** The expected phosphorus and boron profiles in the NW. The P profile was simulated by TRIM code, while the B profile was taken from the SIMS measurements of similarly doped Si layers. As can be seen, according to our process, the P and B profiles should cross in the middle of the NW resulting in a depletion region 40 nm long

NW length of 260 nm implying that the  $p$ - $n$  junction should be confined within the length of the NWs.

To confirm the diode behavior of the NWs, we measured their current–voltage ( $I$ - $V$ ) characteristics by contacting them with a Pt/Ir tip mounted to a micro-manipulator inside an SEM. Details of the measurement system can be found elsewhere [13]. The measured  $I$ - $V$  curves of three different  $p$ - $n$  junction NWs along with an unimplanted  $p$ - $i$  NW are shown in Fig. 3a. The details of these NWs are listed in Table 1. The inset of Fig. 3a shows the  $I$ - $V$  curve of the substrate of the NW. As can be seen from Fig. 3a, all the  $p$ - $n$  NWs show excellent rectifying characteristics with an ON/OFF current ratio of 168, 120, and 50, respectively, at  $\pm 1$  volt (see Table 1). In comparison, the unimplanted  $p$ - $i$  NW shows a quasi-Ohmic behavior implying the lack of

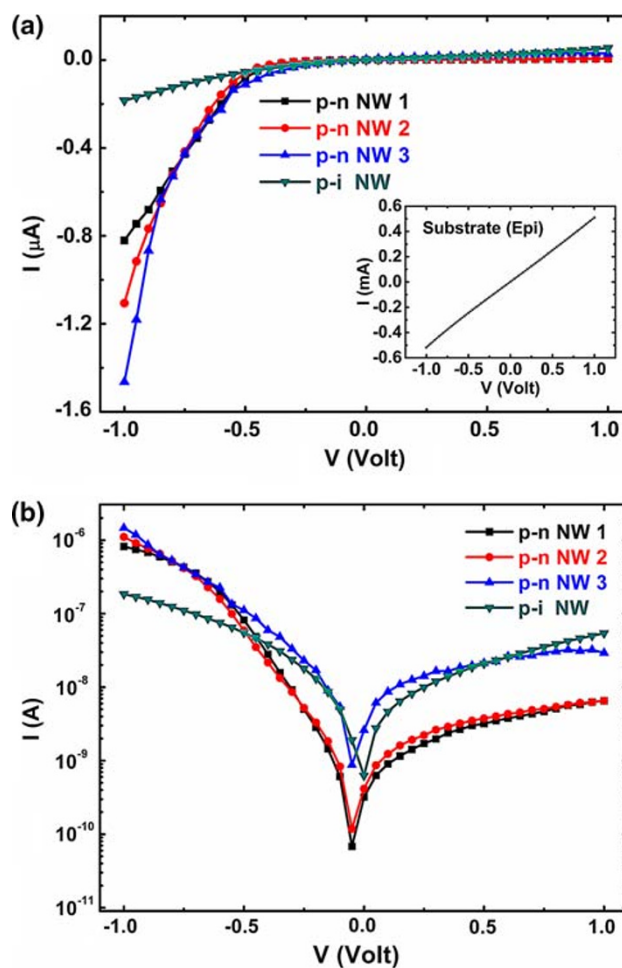


**Fig. 3** The measured electrical current–voltage ( $I$ - $V$ ) characteristics from the NWs. **a**  $I$ - $V$  curves of three  $p$ - $n$  NWs and a  $p$ - $i$  (unimplanted) NW. Please refer to Table 1 for details of the NWs. *Inset* of Fig. 3a shows the  $I$ - $V$  curve of the substrate in the same voltage range. **b** Semi-log plot of the  $I$ - $V$  curves in Fig. 3a. For extracting the ideality factors of the  $p$ - $n$  junctions, the linear regions of the curves of the  $p$ - $n$  NWs in forward bias ( $-0.2$  to  $-0.6$  volt) were used

**Table 1** Details containing the dimensions, the measured ON/OFF current ratios, and ideality factors of the NWs whose  $I$ - $V$  curves are shown in Fig. 3a

Type	Number	Diameter (nm)	Length (nm)	ON/OFF current ratio	Ideality factor (n)
p-n	1	160	250	168	1.8
p-n	2	155	290	125	1.7
p-n	3	230	277	50	2.0
p-i	–	145	280	–	–

The ON/OFF current ratios are calculated at  $\pm 1$  volt

a significantly rectifying junction. The p-type substrate of the implanted NWs (inset of Fig. 3a) showed an Ohmic (linear) behavior. This confirmed that the phosphorus implantation is indeed forming a  $p$ - $n$  junction within the NWs as illustrated in Fig. 2, and it did not extend to the substrate.

In forward bias, the diode current ( $I$ ) in the lower voltage range can be written as [20]

$$I = I_S \left[ \exp\left(\frac{eV}{nk_B T}\right) - 1 \right] \quad (1)$$

where  $I_S$  is the saturation current,  $V$  the applied voltage,  $k_B$  the Boltzmann constant,  $T$  the temperature, and  $n$  the ideality factor of the diode.

We plotted the  $I$ - $V$  curves of Fig. 3a in a semi-log scale in Fig. 3b. From the slope ( $S$ ) of the linear parts of these curves in the lower voltage range ( $-0.2$  to  $-0.6$  volt), we extracted the values of  $n$  by using

$$n = \frac{e}{\ln 10 S k_B T} = \frac{e}{2.3 S k_B T} \quad (2)$$

The values of  $n$  for the three  $p$ - $n$  junction NWs were 2.0, 1.8, and 1.7, respectively (see Table 1). Sah et al. [21] have found that the ideality factor of a  $p$ - $n$  diode can vary from 1 to 4 (or even higher in special cases) depending on what kind of current conduction mechanism is dominating. A value close to 2 for the ideality factor indicates that recombination across the  $p$ - $n$  junction through the surface states is dominant in the carrier transport mechanism. Our  $p$ - $n$  junction NWs are always covered with a 2–3 nm thick native silicon oxide with an estimated surface state density of  $1.1 \times 10^{10} \text{ cm}^{-2}$  [13]. These surface states are in direct contact with the  $p$ - $n$  junction. Therefore we think that surface recombination is indeed playing a major role in the current conduction mechanism across the  $p$ - $n$  junction resulting in the extracted ideality factors close to 2.

## Conclusion

In conclusion, we have demonstrated a novel method to form  $p$ - $n$  junction NW diodes by combining two well-

established doping techniques—in-situ doping and ion implantation, in succession. The measured NWs showed excellent diode characteristics with a high ON/OFF ratio. The ideality factors of the  $p$ - $n$  junctions were close to 2 which points to significant carrier recombinations through the surface states.

**Acknowledgment** The authors thank Mr. A. Frommfield, Mr. K. U. Assmann, Ms. S. Hopfe, and Ms. C. Muexn for technical support. The authors acknowledge the financial support from the FP6 EU project ‘Nanowire based One Dimensional Electronics’ (NODE).

## References

1. M. Law, J. Goldberger, P. Yang, *Annu. Rev. Mater. Res.* **34**, 83 (2004)
2. Y. Li, F. Qian, J. Xiang, C.M. Lieber, *Mater. Today* **9**, 18 (2006)
3. T.J. Kempa, B. Tian, D. Kim, J. Hu, X. Zheng, C.M. Lieber, *Nano Lett.* **8**, 3456 (2008)
4. K.Q. Peng, Y. Xu, Y. Wu, Y. Yan, S.T. Lee, J. Zhu, *Small* **1**, 1062 (2005)
5. Y. Rangineni, C. Qi, G. Goncher, R. Solanki, K. Langworthy, *J. Nanosci. Nanotechnol.* **8**, 2419 (2008)
6. E. Tutuc, J. Appenzeller, M.C. Reuter, S. Guha, *Nano Lett.* **6**, 2070 (2006)
7. S.K. Gandhi, *VLSI Fabrication Principles, Chapt. 6*, 2nd edn. (John-Wiley & Sons, 1994), pp. 368–450
8. G.M. Cohen, M.J. Rooks, J.O. Chu, S.E. Laux, P.M. Solomon, J.A. Ott, R.J. Miller, W. Haensch, *Appl. Phys. Lett.* **90**, 233110 (2007)
9. A. Colli, A. Fasoli, C. Ronning, S. Pisana, S. Piscanec, C.A. Ferrari, *Nano Lett.* **8**, 2188 (2008)
10. K.S. Jones, S. Prussin, E.R. Weber, *Appl. Phys. A* **45**, 1 (1988)
11. R. Duffy, M.J.H. Van Dal, B.J. Pawlak, M. Kaiser, R.G.R. Weemaes, B. Degroote, E. Kunnen, E. Altamirano, *Appl. Phys. Lett.* **90**, 241912 (2007)
12. P. Das Kanungo, R. Kögler, K. Nguyen-Duc, N. Zakharov, P. Werner, U. Gösele, *Nanotechnology* **20**, 165706 (2009)
13. P. Das Kanungo, N. Zakharov, J. Bauer, O. Breitenstein, P. Werner, U. Gösele, *Appl. Phys. Lett.* **92**, 263107 (2008)
14. S. Hoffmann, J. Bauer, C. Ronning, T. Stelzner, J. Michler, C. Ballif, V. Sivakov, S.H. Christiansen, *Nano Lett.* **9**, 1341 (2009)
15. B. Margesin, R. Canteri, S. Solmi, A. Armigliato, F. Baruffaldi, *J. Mater. Res.* **6**, 2353 (1991)
16. S. Solmi, S. Valmorri, R. Canteri, *J. Appl. Phys.* **77**, 2400 (1995)
17. P. Werner, N.D. Zakharov, G. Gerth, L. Schubert, U. Gösele, *Int. J. Mater. Res.* **97**, 1008 (2006)
18. G. Imamura, T. Kawashima, M. Fujii, C. Nishimura, T. Saitoh, S. Hayashi, *Nano Lett.* **8**, 2620 (2008). [www.srim.org](http://www.srim.org)
19. [www.srim.org](http://www.srim.org)
20. S.M. Sze, *Physics of Semiconductor Devices*, 2nd edn. (Wiley, New York, 1981), pp. 63–132
21. C.H. Sah, *IRE Trans. Electron Devices* **ED-9**, 94 (1962)